IET Renewable Power Generation

Research Article

IET Journals
The Institution of Engineering and Technology

Scale model technology for floating offshore wind turbines

ISSN 1752-1416
Received on 9th December 2016
Revised 8th February 2017
Accepted on 24th March 2017
doi: 10.1049/iet-rpg.2016.0956
www.ietdl.org

Ilmas Bayati[1] ✉, Marco Belloli[1], Luca Bernini[1], Hermes Giberti[2], Alberto Zasso[1]

[1]*Department of Mechanical Engineering, Politecnico di Milano, Milano, Italy*
[2]*Universita degli Studi di Pavia, Dip. Ingegneria Industriale e dell'Informazione, Pavia, Italy*
✉ *E-mail: ilmasandrea.bayati@polimi.it*

Abstract: This study illustrates the aerodynamic and mechatronic design of a 1/75 scaled model of the DTU 10 MW wind turbine to perform wind tunnel tests in floating offshore configuration. Due to the strong discrepancy of the Reynolds number between full and model scale (up to 150), a dedicated low-Reynolds airfoil (SD7032) was chosen for the aerodynamic design of the blades, and the final shape was defined based on a dedicated optimisation algorithm which had as target the matching of the scaled thrust force and the first flap-wise bending frequency, as it is thoroughly explained in the study. Furthermore, the mechatronic design is reported in terms of the design choices adopted to get the best target-oriented functionalities to the model (i.e. individual pitch control, bandwidth) and to reduce as much as possible the weights, greatly affecting the aero-elastic scaling. The results gathered during experimental campaigns at Politecnico di Milano wind tunnel, are reported confirming the validity of the design and manufacturing choices.

1 Introduction

Wind energy is significantly growing and consistently with the continuous energy supply demand, moving to multi-megawatt and floating offshore horizontal axis wind turbine's concepts. In this scenario, research and development are playing a key-role in decreasing the overall cost of energy, as well as increasing the efficiency and the reliability of such complex machines. From this perspective, experimental data are necessary for calibrating multidisciplinary and predictive numerical tools, serving also as reference for new generation wind turbines. To this aim, full-scale experiments, which would potentially give the best information, from engineering and operational (decision-making) point of views, suffer from drawbacks such as difficulties in the definition of the inlet boundary condition, along with environmental conditions that are not available 'on request', not to mention the related costs. This brings about the need of a large amount of time to collect a set of data that are representative for the overall operating condition of the machine, beside the non-negligible cost in carrying out these measurements themselves and for such a long period. This generally goes with a limited access to the proprietary data (machine design and wind farms' management data). Wind tunnel tests represent a good solution in that allows to test scale models and to gather reliable data in a controlled environment, with known boundary conditions, making also more consistent the comparison with the numerical counterpart of the same test. In addition, in scale model tests, a large number of different test conditions in shorter amount of time, compared with full scale, allows to cover the whole operational range of the machine. Modern era miniaturised mechatronics, as well as materials technology improvements, allow to build wind tunnel scale model of wind turbine that are very close to the full scale machines, in their functional capabilities. This turns out in testing significant control strategies, (i.e. individual pitch control–IPC), as well as new optimised aero-elastic features.

As the new concepts of multi-megawatt wind turbines are mainly offshore, basin tests are necessary to be combined and compared with wind tunnel tests. However, this brings about some issues in the scaling process. More specifically, Froude number similitude, which characterise ocean basin tests, due to the presence of gravity-based forcing (waves), cannot be adopted in the wind tunnel tests, since it would cause excessively low wind tunnel wind speeds then low measured forces with bad signal/noise ratio (e.g. the velocity scale factor would be $\sqrt{\lambda_L}$ causing a rated wind speed of 1.3 m/s in the tunnel). On the contrary, having higher velocity scale factors, along with the tip speed ratio (TSR) aerodynamic similitude, goes with higher rotational speed of the wind turbine model and then higher frequency band required from the IPC motors for the blade pitch control; therefore a compromise is needed. Furthermore, Reynolds similitude, which is hardly reached in wind tunnel tests, needs handled by scaling blades also accounting for the re-design of the set of the air-foils adopted, trying to optimise the overall thrust of the rotor to be as closest as possible, in terms of similitude, with respect to full scale (e.g. considering the rated condition as the design wind condition without loss of generality for the whole wind speed range).

New advances in testing models of floating offshore wind turbines, in ocean basin and wind tunnel, rely on the hardware-in-the-loop (HIL) approach, which is based on real-time hybrid combination of measurements and simulations [1, 2]. The present research is part of a wider project, LIFES50 + [3], which, among various tasks, aims at investigating thoroughly HIL approach, respectively, at MARINTEK ocean basin [1] and Politecnico di Milano wind tunnel [2, 4]. More specifically, aerodynamic input in ocean basin tests are simulated in real time, as well as the motion of the floating platform for the wind tunnel counterpart, whereas the remainder contributions in terms of forcing are measured, respectively, due to the waves (ocean basin) and the wind (tunnel) on the physical model.

2 Wind turbine scaling process

The DTU 10 MW wind turbine was adopted as the reference for the model described in this paper. The DTU 10 MW was first designed in the framework of the Light Rotor project in 2012 [5], as rational upscale of the NREL 5 MW machine [6]. Then the designed evolved in the current publicly available concept by the DTU wind energy department [7]. At the time of this paper, this concept is widely adopted as the new generation wind turbine reference in various wind energy research activities. The main parameters can be found in Table 1. Given the Politecnico di Milano wind tunnel facility, as the target of this project, the model design starts from the comparison of the turbine specification with the PoliMi Wind Tunnel (GVPM) test section dimensions and capabilities, see [8]. GVPM is a closed circuit facility with two test sections: a 4 × 4 m high speed low turbulence and a 14 × 4 m low

speed boundary layer test section. In the low speed section, the turbulence intensity is circa equal to 2% with a maximum velocity equal to 15 m/s. The low speed section has the main dimension of 36 m length, 14 m width and 4 m height, allowing for very large scale wind engineering simulations, useful for civil engineering application or low blockage aerodynamic related tests. The test section is a boundary layer one, then atmospheric boundary layer is correctly scalable up to 75 scale factor, considering for example the *Eurocode* 0, typically adopted for the definition of wind profile at sea or coastal areas in wind engineering design. All the scaling factors λ_i, as the ratio between the full and model scale quantity, were derived fixing the length and velocity scale factors, defined as λ_L and λ_V, see Table 2. The consistency of choosing separately the length and velocity scale factors comes from neglecting the Froude scaling approach, which, along with keeping the same machine TSR between full and scale model, ends in a dependency of velocity and time scale factors by the length one (i.e. $\sqrt{\lambda_L}$). The reason why Froude scaling can be neglected, contrary to ocean basin tests, is the absence of physical gravitational-based forces as the waves ones during the tests in the wind tunnel. More specifically, the length scale, potentially ranging from 75 to 90, was eventually fixed to 75, in order not to have non-negligible blockage effect but also to avoid excessively miniaturisation of the model components. Furthermore, two different velocity scale factors λ_V, 2 and 3, were considered possible for this application.

3 Aerodynamic design

3.1 Design method

The aerodynamic design for a wind turbine model has the following targets:

Table 1 Turbine scaled parameters

Parameter	Unit	Full scale	$\lambda_V = 2$	$\lambda_V = 3$
cut-in speed	*m/s*	4	2	1.3
rated speed	*m/s*	11.4	5.7	3.8
cut-out speed	*m/s*	25	12.5	8.33
minimum rotor speed	*rpm*	6.0	225	150
maximum rotor speed	*rpm*	9.6	360	240
rotor diameter	*m*	178.3	2.37	2.37
blade length	*m*	86.4	1.15	1.15
hub height	*m*	119	1.58	1.58
blade mass	*kg*	42 E3	0.0995	0.0995
nacelle mass	*kg*	442 E3	1.05	1.05
rotor mass	*kg*	228 E3	0.55	0.55
tower mass	*kg*	628 E3	1.49	1.49
Ct rated	—	0.814	0.814	0.814
Cp rated	—	0.476	0.476	0.476
rated thrust	*N*	1,619,000	72	32
rated torque	*Nm*	10,738,000	6.36	2.82
tilt angle	*deg*	5	5	5

Table 2 Scaling factors

Quantity	Unit	Scaling Factor	Value	
length	*m*	λ_L	75	
speed	*m/s*	λ_V	2	3
rotor speed	*rad/s*	$\lambda_\omega = \lambda_V/\lambda_L$	1/37.5	1/25
frequency	*Hz*	$\lambda_f = \lambda_V/\lambda_L$	1/37.5	1/25
time	*s*	$\lambda_T = \lambda_L/\lambda_V$	37.5	25
acceleration	m/s^2	$\lambda_{acc} = \lambda_L\lambda_f^2$	1/18.75	1/8.3
force	*N*	$\lambda_F = \lambda_V^2\lambda_L^2$	22,500	50,625
moment	*Nm*	$\lambda_F = \lambda_V^2\lambda_L^3$	1,687,500	3,796,875
mass	*kg*	$\lambda_M = \lambda_L^3$	421,875	421,875

- matching the reference aerodynamic thrust coefficient
- matching the reference aerodynamic torque coefficient
- matching the (scaled) first flap-wise blade natural frequency
- matching the (scaled) blade weight

it is evident that this scaling factors, the aero-elastic task is quite challenging. Moreover, for a floating offshore wind turbine, matching the correct scaled thrust force is of greater interest for its contribution in the overall dynamics of the floater [9, 10]. In Fig. 1 the optimal aerodynamic design scheme is reported, showing inputs and outputs of the process. As anticipated, the very low Reynolds number compared with full scale (150 times), required the adoption of dedicated airfoils and to reach a completely different shape of the blade [i.e. model chord c, twist Θ, and thickness over chord (t/c)] as well as structural design. To overcome the Reynolds discrepancy, the SDxx Selig–Donovan low Reynolds database was chosen [11] and the SD7032 was adopted also considering similar previous experiences [9, 10, 12, 13]. In Fig. 2, it can be easily seen the difference in terms of relative thickness (t/c) between the SD7032 airfoil, circa 10% and a sample from the full scale airfoils (FFA-W3-240), ∼24%. Aerodynamic coefficients for the SD7032 for Reynolds numbers equal to 100E3 and 300E3 are available in [11]; however, to obtain a larger database for the aerodynamic design, wind tunnel tests were performed on a 2D section model of the SD7032. This 2D sectional model was manufactured with the same carbon fibre technology used for the final turbine blade model, to ensure a correct reproduction of surface finish effect and to gather as reliable as possible data. Furthermore the wind tunnel sectional tests was equipped with a dynamometer and pressure taps (up to 30) at the mid span, so that drag coefficients and lift coefficients were gathered, respectively, from wake and pressure measurements. In Fig. 3 the experimental results are reported for the following Reynolds numbers 50E3, 60E3, 75E3, 100E3, 125E3, 150E3, 200E3 and 250E3, which are the ones experienced by the airfoils along the blade in the whole wind speed range during the tests.

The design process (Fig. 1) can be summarised as follows

i. Computing model airfoil lift coefficient and its derivative with respect to the angle of attack and drag coefficient from model section characteristics.
ii. Calculating model chord and twist to ensure the target scaled thrust force.
iii. Estimating the mechanical properties of each section.
iv. Optimising for the blade structural design for best 1st flapwise frequency matching.
v. Updating blade section shape and lift coefficient and loop from (i).

and gives as output the optimal blade shape in terms of aero-elastic scaling, considering a velocity scale factor $\lambda_V = 2$. Fig. 4 reports iteration loops, starting from the reference DTU 10 MW up to the final solution for the chord, twist and relative thickness. It is visible how the chord grows higher than the full scale, in particular near the maximum chord position, the twist is almost equally reduced along the blade and the t/c curve goes faster to the tip airfoil value (10%) than the 10 MW one, consistently with the choice of different Reynolds number and airfoils (efficiency) with respect to the full scale blade. Further details of this procedure can be found in [14]. At this point the final shape was converted to a 3D CAD format to create the aluminium mould by CNC manufacturing, being used afterwards for to build the physical *pre-preg* carbon fibre blades (i.e. fibres pre-impregnated by polymer matrix) by means of autoclave process.

3.2 Design verification

The goodness of the design procedure was verified numerically by a blade element momentum (BEM) code. The calculations were performed considering stationary and uniform flow, i.e. without wind shear and turbulence, and considering the turbine structure as completely rigid, also the blade pre-bend and rotor cone angle were

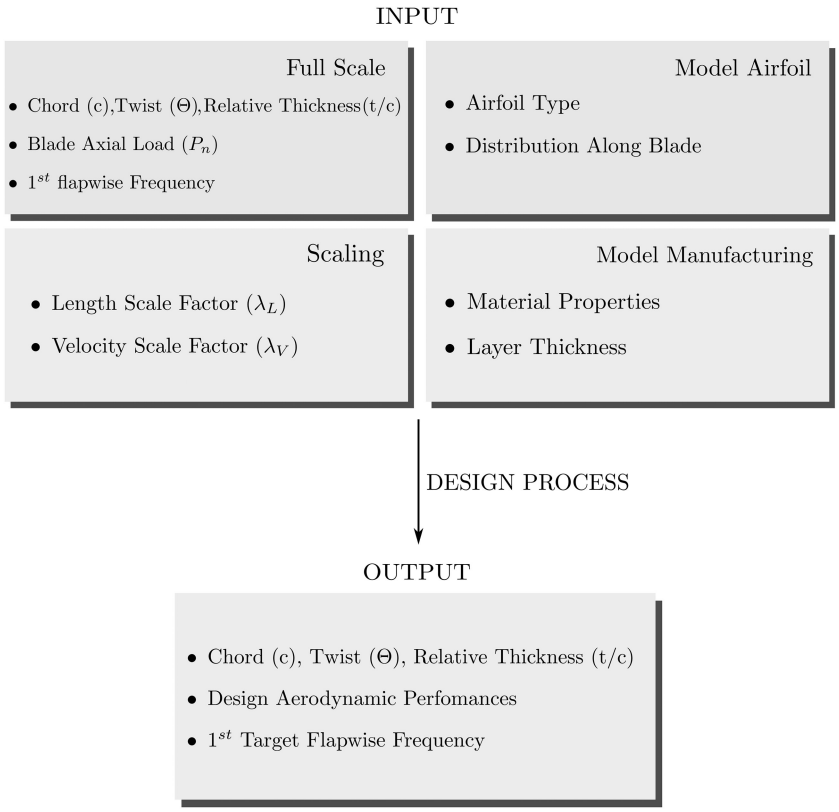

Fig. 1 *Aerodynamic design scheme*

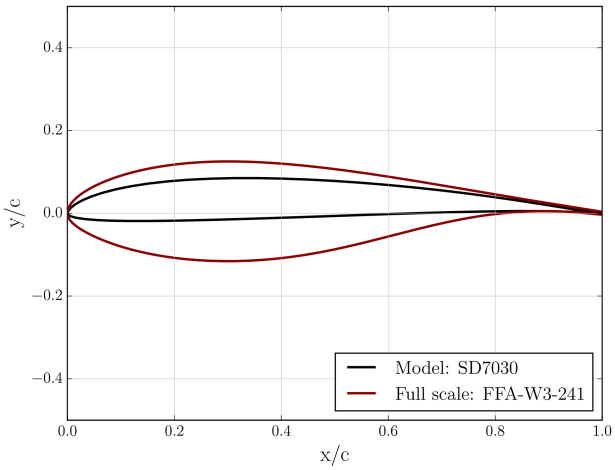

Fig. 2 *Low Reynolds model vs full scale airfoils*

not considered, with the aim of having a fast but reliable simplified design tool. The computed thrust and power coefficient are reported in Fig. 5. It can be seen that the thrust coefficient C_T is well matched by the design, which is the main target for a floating offshore wind turbine scale model. Only for a limited range of TSR (λ) a small discrepancy is evident, whereas the power coefficient C_P has a higher discrepancy for high λ, due to low efficiency of the airfoil itself compared with full scale. However this is not considered an issue for this specific experiment.

4 Mechatronic design

Given the scale factors in Table 2, the structural properties of the wind turbine are easily derived. It is however evident how constrictive the mass scale factor is (Table 1), which depends only on the length scale factor λ_L, for a physical model to be designed and built. When it comes to modelling a highly electrically equipped system like this, this constraint is even heavier due to commercial components (e.g. motors, controllers, and cables)

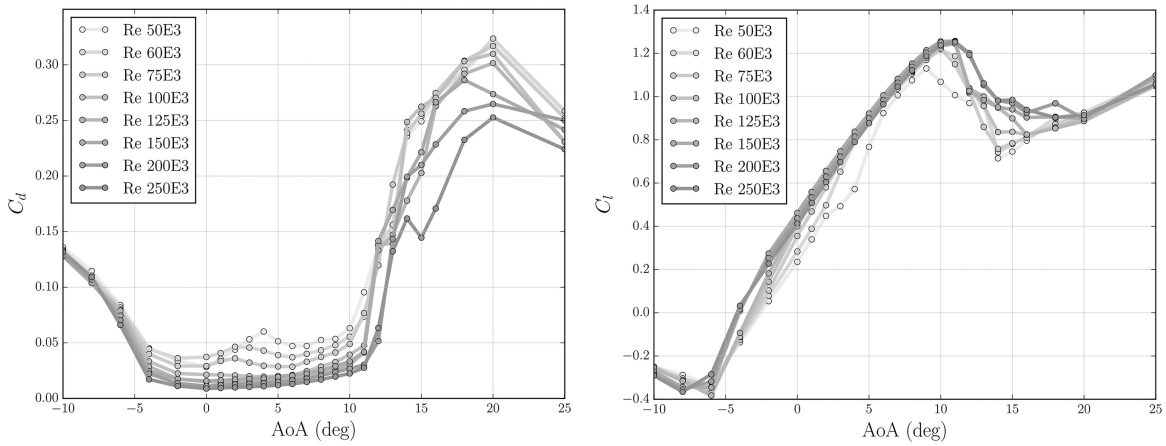

Fig. 3 *Experimental aerodynamic coefficients: Lift coefficient C_l from pressure measurements (left-hand side), Drag coefficient C_d from force measurements (right-hand side)*

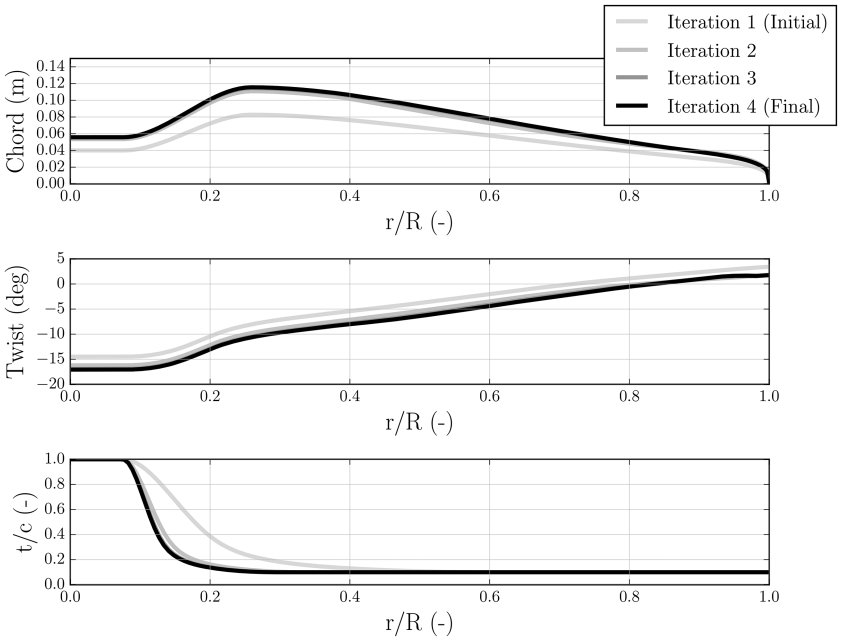

Fig. 4 *Blade design iterations*

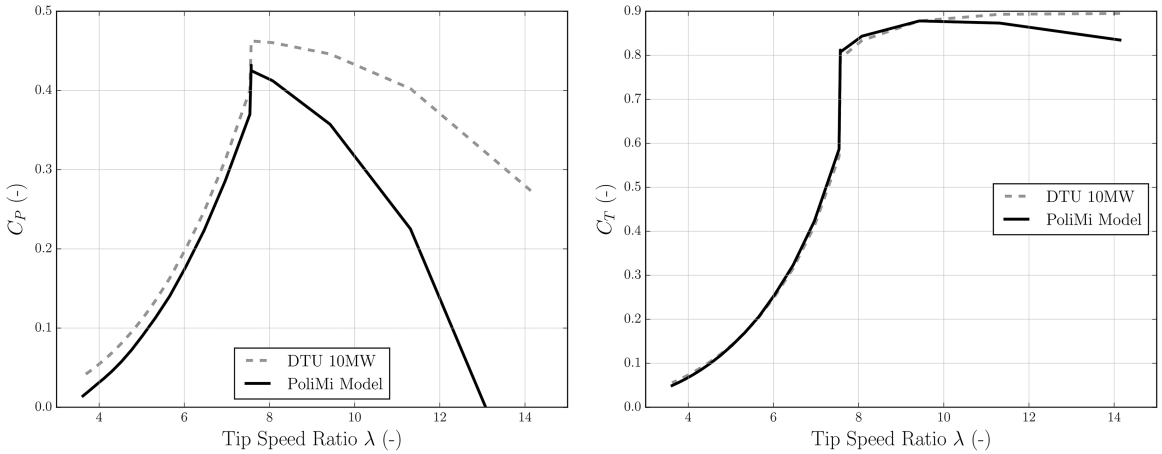

Fig. 5 *Model vs full scale performance (numerical computations): Power Coefficient C_T (left-hand side), Thrust Coefficient C_P (right-hand side)*

which cannot be customised. Therefore, the weight of these elements, along with commercial mechanical parts as couplings and connectors, turn out to represent the great part of the overall mass of an IPC wind turbine model as this.

The mechanical design of the wind turbine scale model can be divided into three functional subgroups:

- *Nacelle*: the main shaft motor is misaligned with respect to the main shaft and the coupling is realised by means of toothed belt transmission. Moreover, a rotary slip ring unit was necessary to ensure the connection to the IPC motors, in terms of power supply and digital/analogue signals input/output, respectively, from the master controller and the acquisition system.
- *Rotor*: this subgroup, supported by the nacelle, is divided, in turn, in blades and hub. The latter bears the IPC control mechanism equipped with single blade motor-reducer units.
- *Tower top*: this subgroup is the connecting element between the tower and the nacelle and it is composed of a six-axis dynamometric balance to measure the aerodynamic forces on the rotor.

4.1 Nacelle

The nacelle unit is shown in Fig. 6. It is characterised by a '*U*' shaped structure, made of high modulus carbon fibre. This structure ensures the correct positioning of the main shaft motor, of the slip ring and of the main shaft, which is connected to the rotor. In addition, the bottom surface of this element is directly connected to the six-axes load balance of the *tower top* unit. The fore surface is inclined in order to guarantee the prescribed 5° tilt angle of the main shaft. The reason of a hollowed main shaft and the principal motor on two different axes is to allow the electrical cables coming from the slip ring to reach the drives of the IPC motors. Another innovative feature is the system used to support both the main shaft and the pulley to which the principal motor is connected: cross-roller bearings have been adopted, since they allow to save space and to bear very high bending moments with the same weight of a single ball bearing. The usage of ball bearings would require two of these elements for each axis, leading to a bigger structure and to an increase of weight. Two aluminium cases directly glued to the carbon fibre structure are devoted to hold the external cup of the cross-roller bearings. As mentioned, the transmission of the motion from the principal motor to the main shaft is realised by means of a toothed belt that introduces a transmission ratio equal to 2. The idea of using a gear-to-gear coupling was discarded because it would have led to an excessive increment of mass. Taking into account the specifications and the transmission ratio introduced by the toothed belt, the principal motor was to have at rated, for a $\lambda_V = 2$ (Fig. 2), the following capabilities: $T = 2.15$ Nm and $\Omega = 720$ rpm, respectively in terms of torque and angular velocity at rotor. In general, it is not difficult to find a commercial solution that meets these characteristics, but the restrictions on the mass considerably reduced the possible candidates. The best solution turned out to be a brushless DC motor EC-4 Pole 30 by Maxon

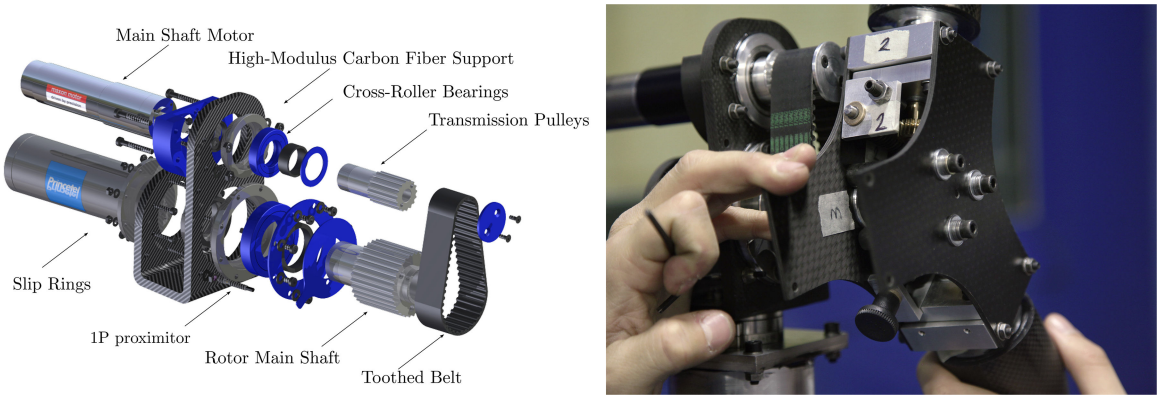

Fig. 6 *Nacelle exploded view (left-hand side) and assembly (right-hand side)*

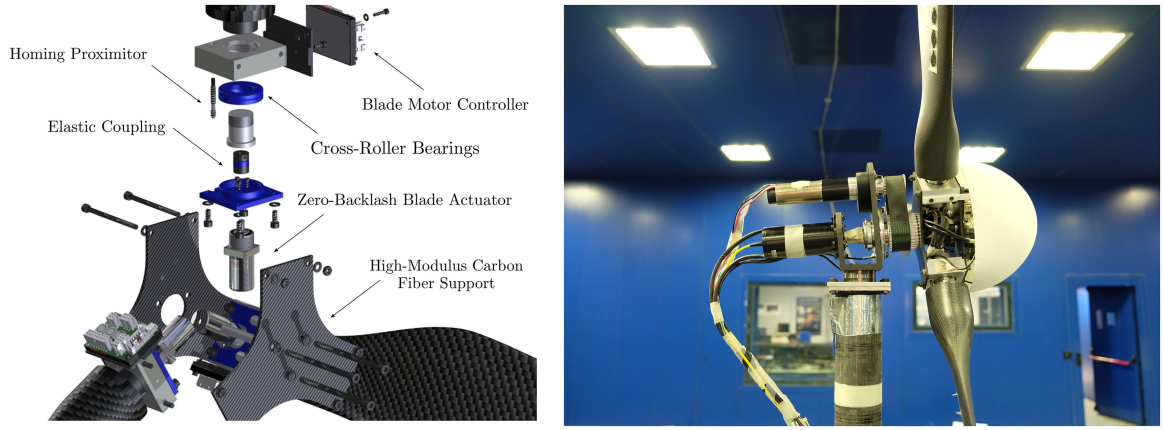

Fig. 7 *Rotor exploded view (left-hand side) and assembly (right-hand side)*

equipped with a GP 32 HP planetary gear with a transmission ratio of 21:1 and a magnetic encoder with a resolution of 500 [1/rpm]. The principal motor is fixed to the carbon fibre structure by means of an ABS support element realised with a 3D printer.

4.2 Rotor

In Fig. 7 the exploded view of the rotor design is reported. It can be seen the structural support of the blades roots is given by two carbon fibre triangular plates and by three aluminium blocks, whose aim is to keep the distance between the two plates, as well as to hold the pitch control mechanisms. To make the hub even stiffer three carbon fibre hollowed spacers are placed between the plates. For this application it is also mandatory to eliminate the risk of vibration phenomena that would invalidate the results. In this regard, it was fundamental to ensure that the hub structure was as stiff as possible in order not to turn the first blade flapwise bending mode into a rigid mode, at lower frequency, merely due to the soft constraint at their roots. Therefore, finite element method (FEM) model was created to verify the non-trivial structural response of a carbon fibre plate coupled with aluminium flange, as the case of the IPC mechanism. design. The FEM model takes into account the presence of the aluminium blocks at the three ends of the hub, whose mass cannot be neglected. Thanks to the high stiffness of the carbon fibre, a width of 3 mm is sufficient to have the frequency associated to the first mode of vibration to 68 Hz, ensuring a greatly higher frequency compared with the first flap-wise blade natural frequency, ~22 Hz, with the design velocity scale factor $\lambda_V = 2$. Regarding the connection between the hub and the blades, the cross-roller bearings turned out to be the best choice to bear the estimated loads at the blade's root, considering the small available space. The related housing for the outer cup is realised within the aluminium blocks, and the blockage is guaranteed by a flange.

The IPC motor reducer unit was chosen, by means of the procedure explained in [15], considering to be able to perform an amplitude of 5° at 1P frequency with respect to the main shaft angular speed at rated which means, considering $\lambda_V = 2$, an angular speed of $\Omega = 360$ rpm. The mentioned procedure is helpful in choosing the optimal motor-reducer combination among a user defined database, also considering the load characteristics in terms of the so called *load* and *acceleration* factors, which are mostly affected by inertial terms rather than the aerodynamics. The optimal choice turned out to be a miniaturised zero-backlash harmonic drive (HD RSF supermini 5B). More details for the nacelle and the rotor design can be found in [16].

5 Experimental verification

5.1 Modal analysis

After the building process was completed, an experimental modal analysis was required to verify the effective natural frequencies of the model, up to the frequency range limit effectively considered involved in the aero-elastic behaviour during experiments; moreover, since the manufacturing and building process bring about some inevitable uncertainties, this verification is also fundamental to slightly modify afterwards the velocity (and frequency) scale factors, before defining the wind tunnel test conditions, in order to be as consistent as possible in the results up-scaling process. The following mode shapes were investigated: 1st isolated blade flap, 1st tower fore-aft and 1st blade collective flap (Fig. 8). The results are reported in Table 3, showing good results for a frequency scale factor $\lambda_f = 1/25$ (see Table 2). It is worth mentioning that, at the time of this paper, a new version of the wind turbine model reported is being mounted. This second version has been designed with the specific target of further decreasing the overall mass of the nacelle, adopting an advanced design approach to face the highly constrictive issue of the model mass target. Therefore, the results shown in Table 2 are expected to increase the 1st tower fore-aft frequency and decreasing the discrepancy.

5.2 Wind tunnel

Wind tunnel experiments were carried out to verify also the aerodynamic design and also as a preliminary activity with respect

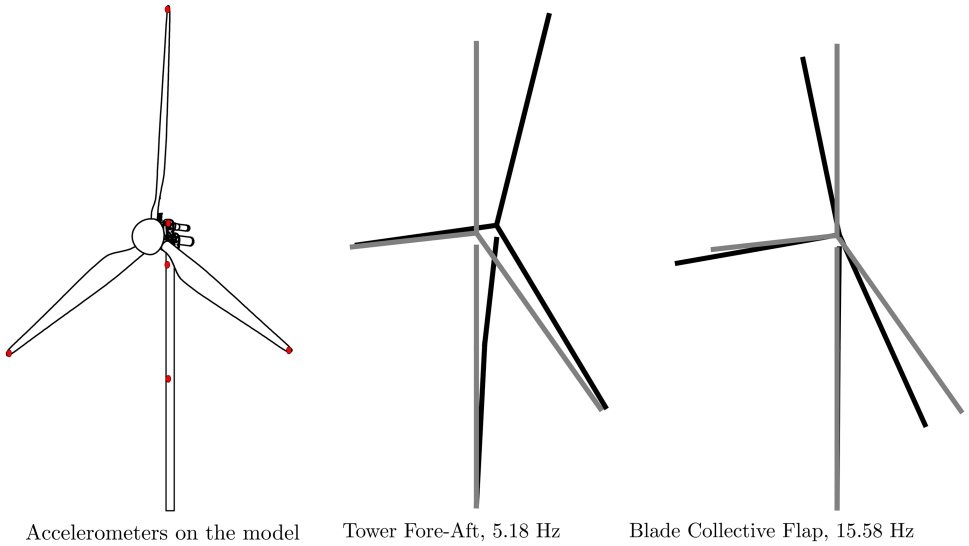

Fig. 8 *Modal analysis results about the whole wind turbine model*

Table 3 Wind turbine model: natural frequencies verification

Mode	Full scale, Hz	Target ($\lambda_f = 1/25$)	Model
1st tower fore-Aft	0.251	6.275	5.18
1st isolated blade flap	0.61	15.25	17.1
1st blade collective flap	0.634	15.85	15.58

to [17]. In Figs. 9 and 10 the thrust and torque measurements in smooth flow conditions are reported, for two different velocity scale factors λ_V. Fig. 9 is related to the tests performed with $\lambda_V = 2$, consistently with the aerodynamic design target (Fig. 1), showing a very good agreement both for thrust and torque; whereas Fig. 10 reports the results performed at $\lambda_V = 3$. More specifically, due to an aerodynamic condition different from the design one the values measured by the model are lower than the full scale target; nevertheless, imposing a variation of the blade pitch angle ϕ the discrepancy between the effective thrust force and the target is eliminated, although without a sound improvement of the torque, due to a less efficient profile compared with the full scale airfoils. In fact it SD7032 airfoil was chosen for its linear lift coefficient C_l before the stall region (Fig. 3) at low Reynolds numbers rather than its lift over drag coefficient (C_l/C_d, efficiency). Nevertheless, with this blade pitch angle correction, the thrust force is matched anyway, also for this velocity scale factor, which is fundamental for this specific offshore purpose. This velocity scale factor is also consistent with the effective aero-elastic scaling of the model (Table 3).

6 Conclusions

This paper presented the methodological approach, the effective design and the realisation of an offshore wind turbine scale model for wind tunnel tests, discussing the critical aspect and the design choices, in terms aerodynamics and mechatronics. Also wind tunnel test results as a verification of the effective aerodynamic performance are reported for two different velocity scale factors. The aerodynamic design was based on the adoption of a low Reynolds airfoil (SD7032) and the final blade design was reached through an optimised aero-elastic distribution to match the target scaled thrust and the first flapwise natural frequency. For a machine like, this with IPC control purposes, the scaling design and realisation is even harder due to the high constraints in terms of mass, however good results have are shown out of the modal analysis reported, considering also room of further improvements with the second version of the wind turbine model being finalised at the time of this paper. Wind tunnel tests results also show very good agreement between the measurements and the target, in terms of thrust and torque for the design velocity scale factor. A different scale factor requires a modification in the blade pitch angle with respect to the full scale to tune the thrust, which is the main target for a floating offshore system, to the desired value. Therefore, although considering initially a velocity scale factor $\lambda_V = 2$, upon which the aerodynamic design has been targeted, related to a frequency scale factor $\lambda_F = 1/37.5$, this turned out to be hardly reachable due to mechanical reasons. Nevertheless, $\lambda_V = 3$ ($\lambda_F = 1/25$) is compatible with the effective realisation of the model in terms of the aero-elastic design.

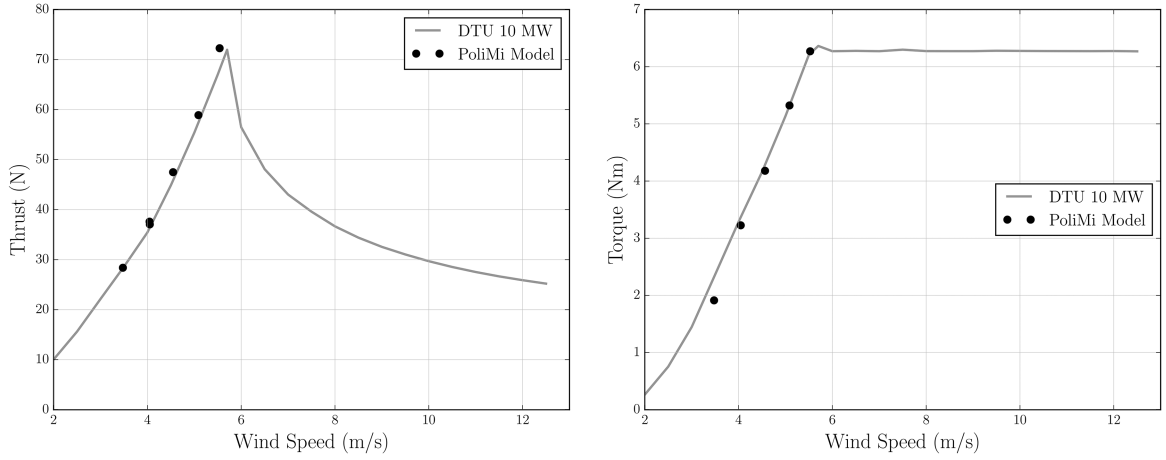

Fig. 9 *Wind tunnel test results, for $\lambda_V = 2$: thrust (left-hand side) and torque (right-hand side)*

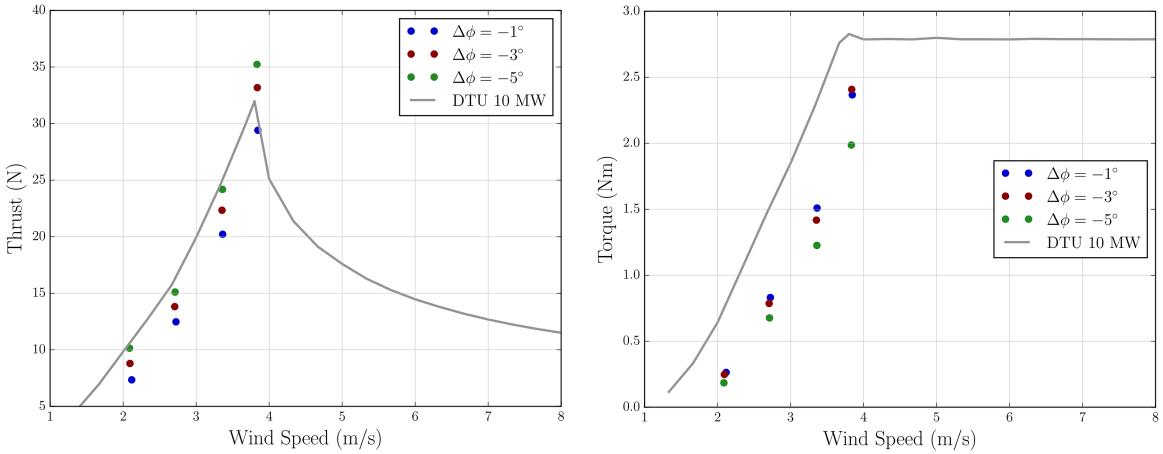

Fig. 10 *Wind tunnel test results, for $\lambda_V = 3$: thrust (left-hand side) and torque (right-hand side), for different variation of the blade pitch angle ($\Delta\phi$) with respect to the full scale nominal value*

7 Acknowledgments

This project has received funding from the European Union's Horizon 2020 research and innovation programme under grant agreement no 640741.

8 References

[1] Bachynski, E., Chabaud, V., Sauder, T.: 'Real-time hybrid model testing of floating wind turbines: sensitivity to limited actuation', *Energy Procedia*, 2015, **80**, pp. 2–12, doi: 10.1016/j.egypro.2015.11.400

[2] Bayati, I., Belloli, M., Facchinetti, A., *et al.*: 'Wind tunnel tests on floating offshore wind turbines: A proposal for hardware-in-the-loop approach to validate numerical codes', *Wind Eng.*, 2013, **37**, (6), pp. 557–568, doi: 10.1260/0309-524X.37.6.557

[3] H2020 Lifes50 + Project official website. Available at http://lifes50plus.eu

[4] Bayati, I., Belloli, M., Ferrari, D., *et al.*: 'Design of a 6-DoF robotic platform for wind tunnel tests of floating wind turbines', *Energy Procedia*, 2014, **53**, pp. 313–323

[5] Bak, C., Bitsche, R., Yde, A., *et al.*: 'Light rotor: The 10-MW reference wind turbine'. Proc. of EWEA 2012 – European Wind Energy Conf.

[6] Jonkman, J., Butterfield, S., Musial, W., *et al.*: 'Definition of a 5-MW reference wind turbine for off-shore system development'. Technical Report NREL/TP-500-38060, NREL, National Renewable Energy Laboratory, 2009

[7] Bak, C., Zahle, F., Bitsche, R., *et al.*: 'The DTU 10-MW reference wind turbine [Sound/Visual production (digital)]'. Danish Wind Power Research 2013, Fredericia, Denmark

[8] Zasso, A., Giappino, S., Muggiasca, S., *et al.*: 'Optimization of the boundary layer characteristics simulated at Politecnico di Milano boundary layer wind tunnel in a wide scale ratio ranges'. IRIS Politecnico di Milano, 2005

[9] Bredmose, H.: 'Contribution to InnWind Deliverable 4.22, scaling laws for oating wind turbine testing'. DTU Wind Energy, 2014

[10] Bredmose, H., Mikkelsen, R., Hansen, A.M., *et al.*: 'Experimental study of the DTU 10 MW wind turbine on a TLP floater in waves and wind'. EWEA Offshore 2015 Conf., Copenhagen, 2015

[11] Lyon, C.A., Broeren, A.P., Gigure, P., *et al.*: '*Summary of low-speed airfoil data*' (SoarTech Publications), **3**

[12] Bottasso, C., Campagnolo, F., Petrovic, V.: 'Wind tunnel testing of scaled wind turbine models: beyond aerodynamics', *J. Wind Eng. Ind. Aerodyn.*, 2014, **127**, pp. 11–28

[13] Campagnolo, F., Bottasso, C., Bettini, P.: 'Design, manufacturing and characterization of aero-elastically scaled wind turbine blades for testing active and passive load alleviation techniques within a ABL wind tunnel'. The Science of Making Torque from Wind, 2014, Virginia Beach, VA, 1998

[14] Bayati, I., Belloli, M., Bernini, L., *et al.*: 'On the aero-elastic design of the DTU 10MW wind turbine blade for the LIFES50 + wind tunnel scale model', *J. Phys. Conf. Series*, 2016, **753**, (2), doi: 10.1088/1742-6596/753/2/022028

[15] Giberti, H., Cinquemani, S., Legnani, G.: 'A practical approach to the selection of the motor-reducer unit in electric drive systems mechanics based design of structures and machines, 2011, **39**, (3), pp. 303–319

[16] Bayati, I., Belloli, M., Bernini, L., *et al.*: 'On the functional design of the DTU10 MW wind turbine scale model of LIFES50 + project', *J. Phys. Conf. Series*, 2016, **753**, (5), doi: 10.1088/1742-6596/753/5/052018

[17] Bayati, I., Belloli, M., Bernini, L., *et al.*: 'Wind tunnel validation of AeroDyn, within LIFES50 + project: imposed surge and pitch tests', *J. Phys. Conf. Series*, 2016, **753**, (5), doi:10.1088/1742-6596/753/9/092001